



Analysis of the dynamic behavior of the cracked stepped shaft used in the rotating equipment

Muhsin. J. Jweeg¹, Salah. N. Alnomani², Salah. K. Mohammad²

¹ Al-Farahidi University, College of Engineering Technology, Iraq.

² University of Kerbala, College of Engineering, Mechanical Engineering Department, Iraq.

Received 1 Aug. 2019; Received in revised form 11 Sep. 2019; Accepted 12 Sep. 2019; Available online 1 Nov. 2019

Abstract

The main objective of this research is to study the impact of cracking on the static and dynamic behavior for the purpose of faults diagnoses. Experimental and numerical analysis techniques were used for an intact shaft and for a cracked one. The natural frequency, dynamic response, equivalent stresses and total deformation of the static and dynamic behavior of uncracked and cracked rotors were detected. Several cracks with different values of depths and locations were performed for this purpose. The ANSYS package was used in numerical analysis to simulate the behavior of cracked shafts during operation and to correlate the vibration effect with the specific cracks on the shaft. The experimental work was completed by manufacturing a test rig consisting of a rotary part to monitor the dynamic behavior of the testing model. The resulting data was recorded and saved by a computer program (SIGVIEW). The effect of the crack on the response, the natural frequency, stress, and the total deformation was determined by measuring the dynamic frequency response and the vibration for each acceleration that will give a pointer to the control system, and to achieve numerical and experimental analysis during the study of centrifugal pumps and steam turbines. Results show a good agreement between numerical and experimental analyses, it was found that the maximum variance was equal to (10.55%) for the bending frequencies and (10.51%) for the torsional frequency and the dynamic response increases by 26% to 33% and the critical speed decreases by 15% to 20% at crack depth (12mm), This is very important in the detection and diagnosis of early cracks and sclerosis for the purpose of avoiding catastrophic failure.

Copyright © 2019 International Energy and Environment Foundation - All rights reserved.

Keywords: Crack; Static; Dynamic; Shaft; Numerical analysis.

1. Introduction

Rotational dynamics is a very important and extensive engineering field. It was used in several fields of mechanical engineering's, such as fluid mechanics, solid mechanics, heat transfer, etc. Rotational dynamics were analyzed to control the vibrational energy as little as possible, as well as to ensure stable operation. Dynamic response of external loads, critical speeds, natural frequencies, bending and torsion mode, stability analysis, etc. In the design and operation of rotating equipment and troubleshooting, analysis of rotor dynamics can help achieve the following general objectives:

1. Predict critical velocities.
2. Determine patch blocks and measured vibration data balance.

3. Simultaneous vibration prediction

4. Prediction threshold velocities and vibration frequencies for dynamic instability.

The existence and growth of cracks is a dangerous problem that may lead to stress concentration in rotating shafts and, as a result, will lead to earlier failure. Transverse cracks are perpendicular to the centerline of the shafts, such a crack was represented by a circular sector shape [1]. They may cause large deviations in the rotor, and failures in pregnancy may occur due to the force transferred to the bearings. The rapid rotation of the rotary shaft through critical speed can reduce the capacity of the rotary, while the slow transition during critical speed can lead to large capacity development. As a first step to understanding the nature of a rotary bearing system, the non-inhibitory critical speed modes must be calculated [2]. In the case of resonance, the frequency of the harmonic elements of the cyclic effect phenomenon is equal to or approximates the natural frequency of any method of rotary vibration [3]. It is important to predict the dynamic behavior of rotary systems to ensure effective rotor work efficiency and to help to take the necessary preventive measures, dynamic behavior changes with crack development because it reduces the strength of body and material, as well as vibratory response to the rotating shaft, will change more or less. Rotary equipment monitoring systems may be developed online to detect cracks since the cleft shaft creates vibrations so monitoring the vibration is more important to detect a crack in the shaft [4, 5]. Usually, the location of the resonance mode can be accurately estimated in the systems by numerical analysis, but this analysis does not give a clear relationship between the frequency and the amount of stiffness and damping [6]. In all rotors and for all operating speeds it is impossible to keep the rotor fully balanced so that the resulting vibration due to the rotor imbalance is always present, and it is necessary to reduce the imbalance as much as possible and not completely eliminate it [7]. There are two types of whirling, forward and backward, as shown in Figure 1, (a) Forward whirling was obtained when the whirling direction is the same as the rotational speed direction of rotary systems, and this type is more dangerous because it is easy to trigger the resonance with the primary rotation. On the other side, (b) backward whirling was obtained when the whirling direction is opposite the rotational speed direction, the frequencies of these whirling motion called natural whirling frequencies [8].

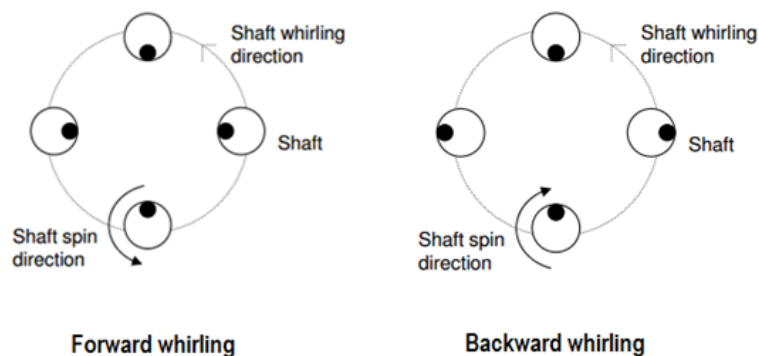


Figure 1. Forward and backward whirling [8].

Due to the presence of cracks in the rotor, many changes occur in natural frequency. These changes depend on the size and location of the cracks on the shaft so that increasing the crack depth reduces the natural frequency of the cracked shaft for all vibration modes [9, 10]. It is necessary to use a coupling to align the shaft with the motor shaft and bearings to ensure that the center was aligned to the center for the purpose of minimizing the misalignment effect of engine vibration and interfering with the rotor response [11]. The hardness of the bearings and the speed of rotation have a great effect on the natural frequencies. This is evident through the numerical model. The increase in the rotational speed reduces the rotation frequency and the speed of the threshold for instability [12].

2. Experimental investigation

A test rig was designed to simulate the centrifugal pump used in some oil industries. This rig consists of a variable diameters steel stepped shaft that was manufactured with a density of (7850 kg/m^3) and Young's modulus of ($210 \times 10^9 \text{ N/m}^2$). The total length of the stepped shaft was prepared to be (404mm) with a mass of (2.19kg). This shaft was supported by two ball bearings and a rotor disc (impeller) with a diameter of (100mm) and a mass of (2.5kg) was connected to the free end (A) of the rotary shaft as can be seen in

Figure 2. An electrical driving motor of (1.5 kW) was coupled by flexible coupling at (B) to drive the shaft. A suitable accelerometer was used with an analyzer of type FFT for vibration signals, [13-15]. Vibration signals were measured at six different rotational speeds (500,1000,1500,2000,2500, and 3000 rpm). The rotational speed was measured by the digital tachometer, while the test rig was operated for a few minutes to settling minor vibrations. As can be seen, in the experimental work, the test rig was designed by connecting all equipment such as data acquisition, the amplifier, digital oscilloscope, accelerometer and, the speed control unit with the speed measurement connected to the computer that works with the SIGVIEW software as shown in Figure 3. SIGVIEW program was used to analyze and draw the estimated signals coming from the oscilloscope, [16, 17].

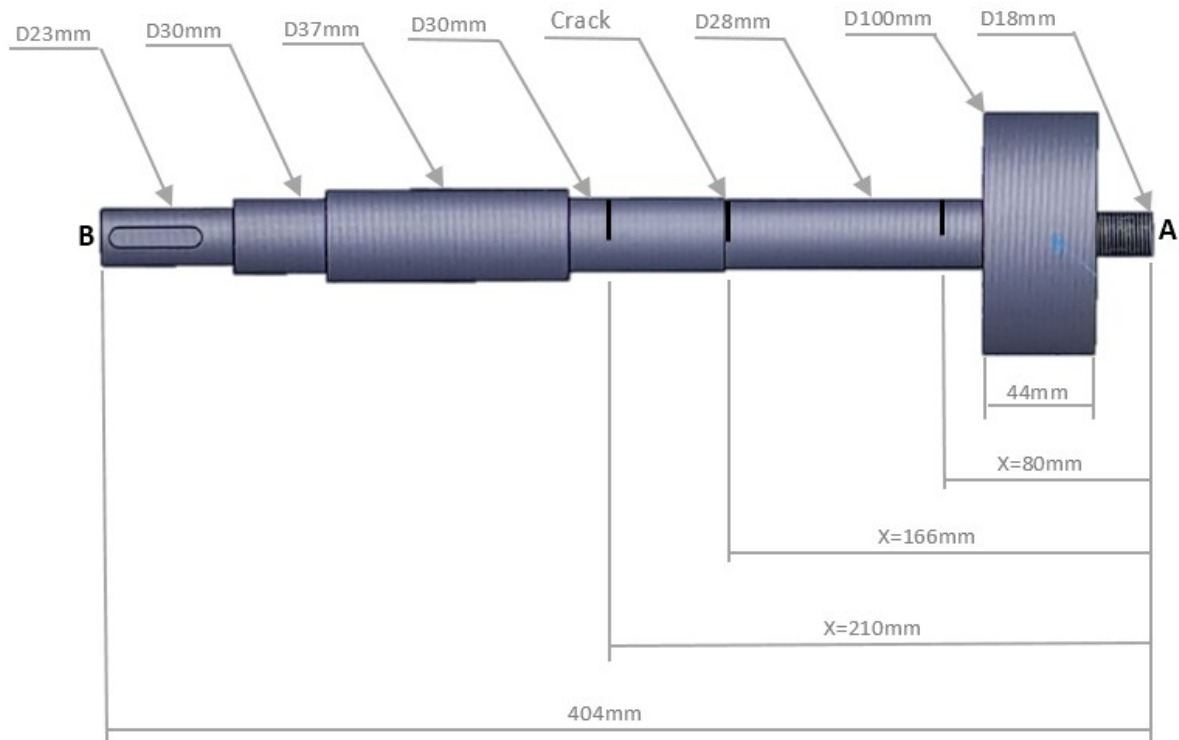


Figure 2. Crack positions on the shaft model.

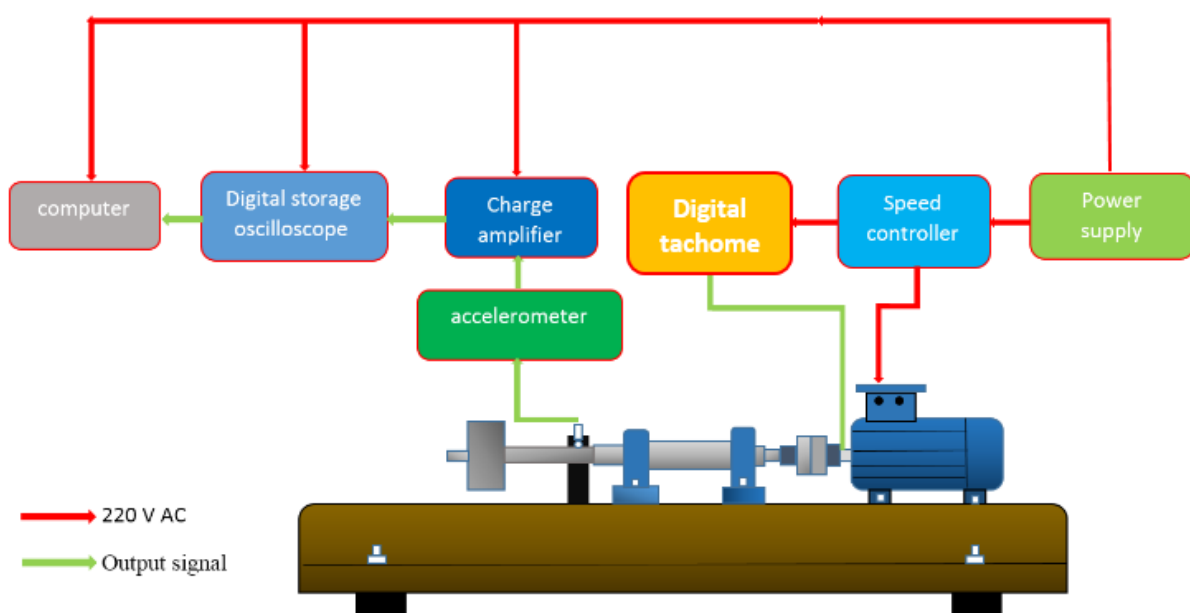


Figure 3. Instrumentation schematic diagram.

Figure 4, illustrates the test rig that was used to obtain data and experimental results. Cracks were detected at the early stage of propagation by comparing the change in response and the critical speed with depth estimation. Experiments were performed on the intact shaft and cracked shaft with a transverse crack. Transverse crack was made in the stepped shaft using a suitable cutting tool with depths (4mm, 6mm, 8mm, 10mm, and 12mm) at different locations on the shaft ($x = 80\text{mm}$, $x = 166\text{mm}$ and $x = 210\text{mm}$) to examine their impact on the response and natural frequency of the system at different rotations (500, 1000, 1500, 2000, 2500), and 3000) Rpm.

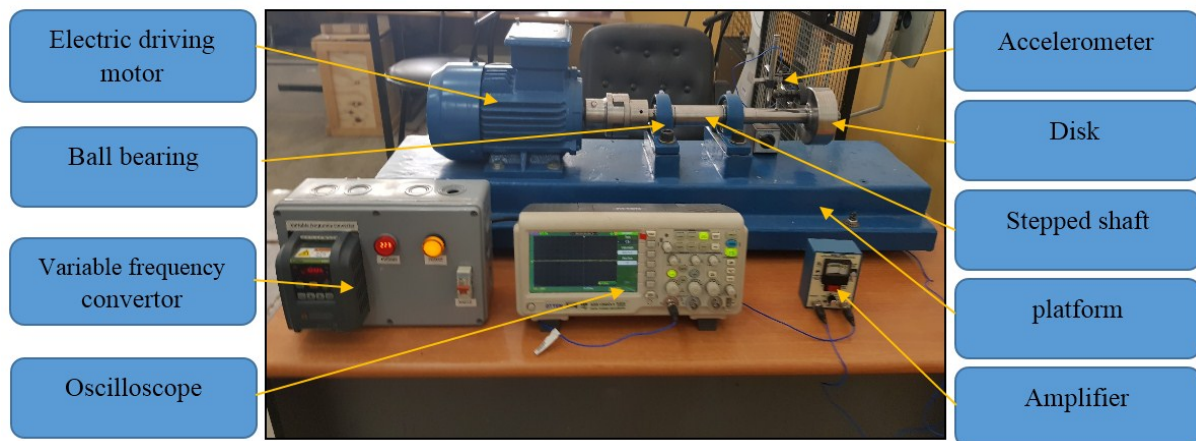


Figure 4. Experimental test rig for the tested stepped shafts.

3. Numerical investigation

ANSYS workbench 16.0 package was used for conducting the numerical analysis to simulate the tested modules [18, 19], as shown in Figures (5 and 6). The using of the finite element method is very useful to indicate fundamental natural frequency, [20], total deformation, [21-25], equivalent stresses, [26-32], and the dynamic response for isotropic stepped shaft at a certain size, the type of element and the type of mesh are selected [33-35]. The meshing was done using a tetrahedron [36-38], (automatic meshing) for the shaft and the disc. In detail, the mesh size was (0.9mm) for getting regarding (76417) elements and (129600) nods for the intact shaft and regarding (76694) elements and (130001) nods for the cracked shaft as shown in Figures (7 and 8).

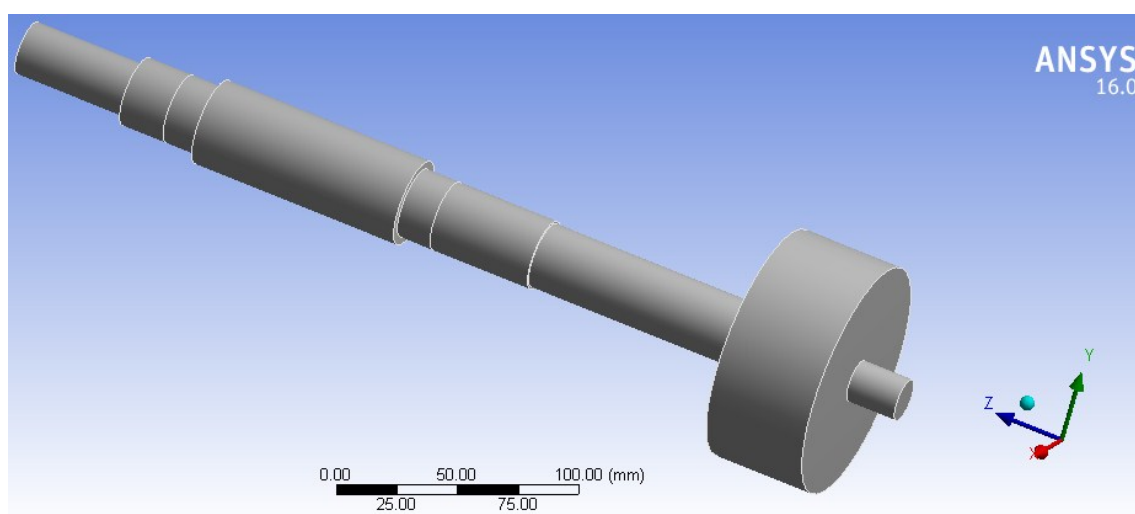


Figure 5. Intact shaft with disc.

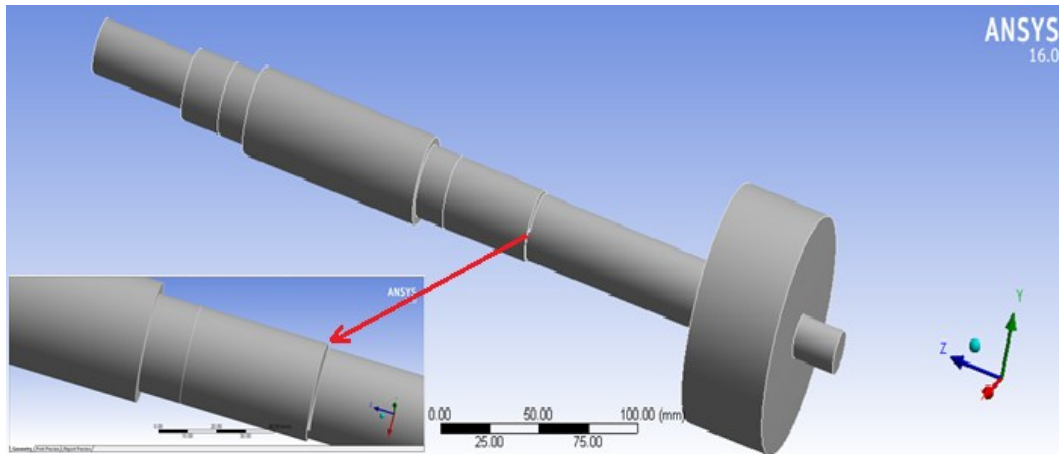


Figure 6. Cracked shaft with disc.

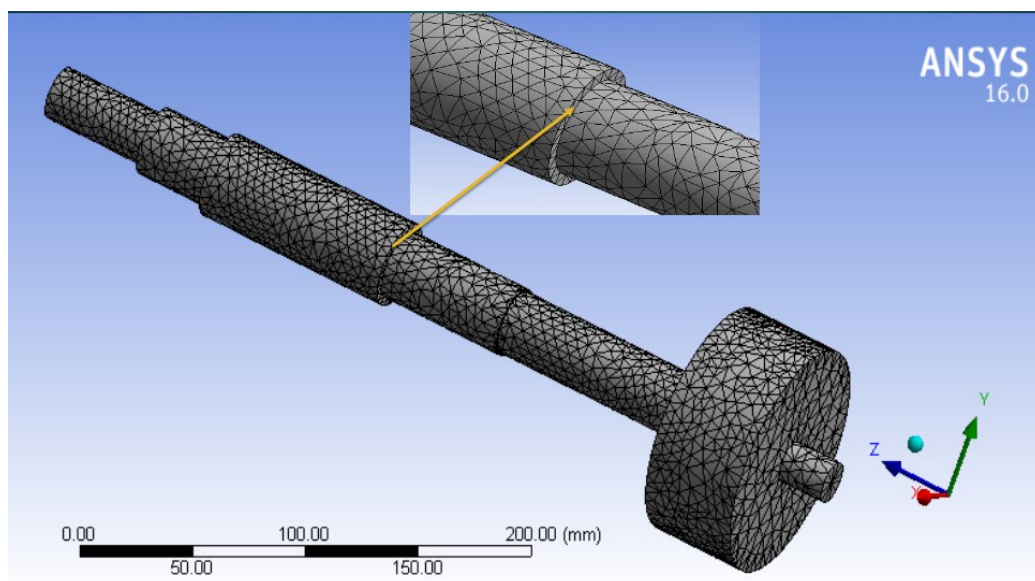


Figure 7. Meshed intact model.

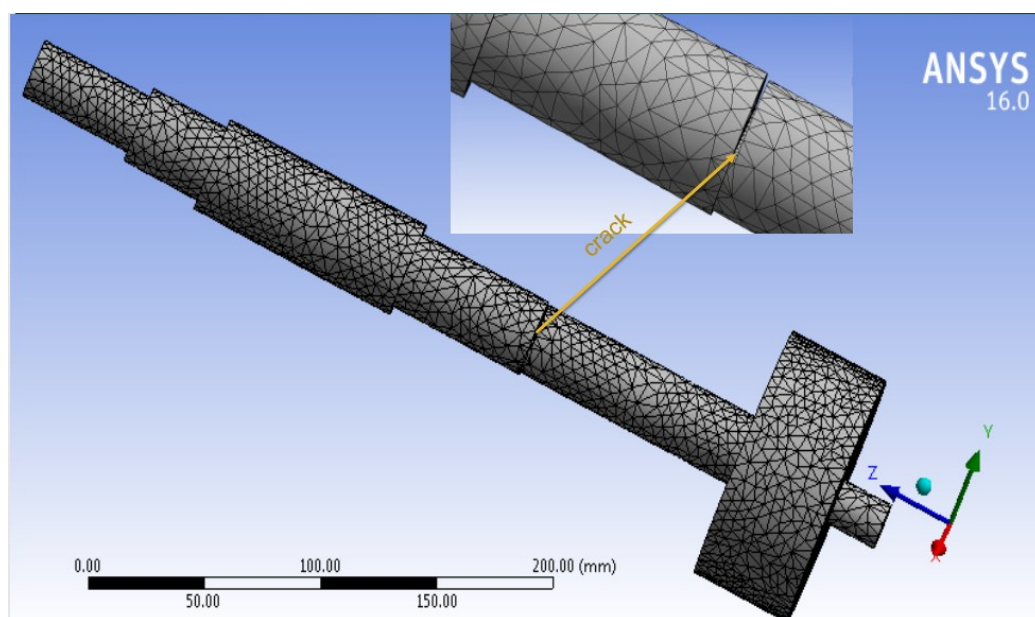


Figure 8. Meshed cracked model.

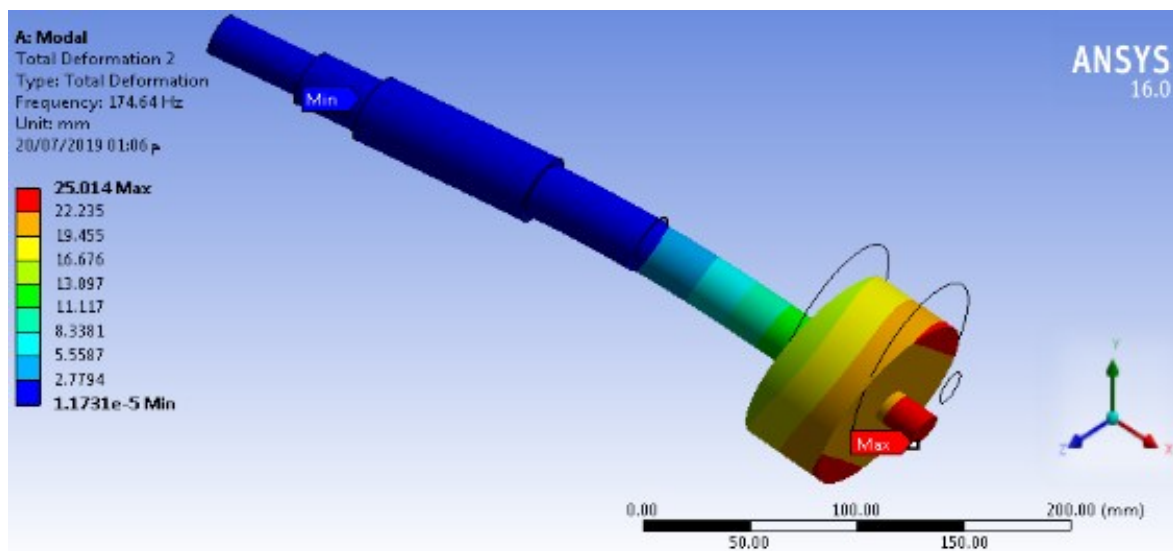
4. Results and discussions

4.1 Results for Uncracked stepped shaft

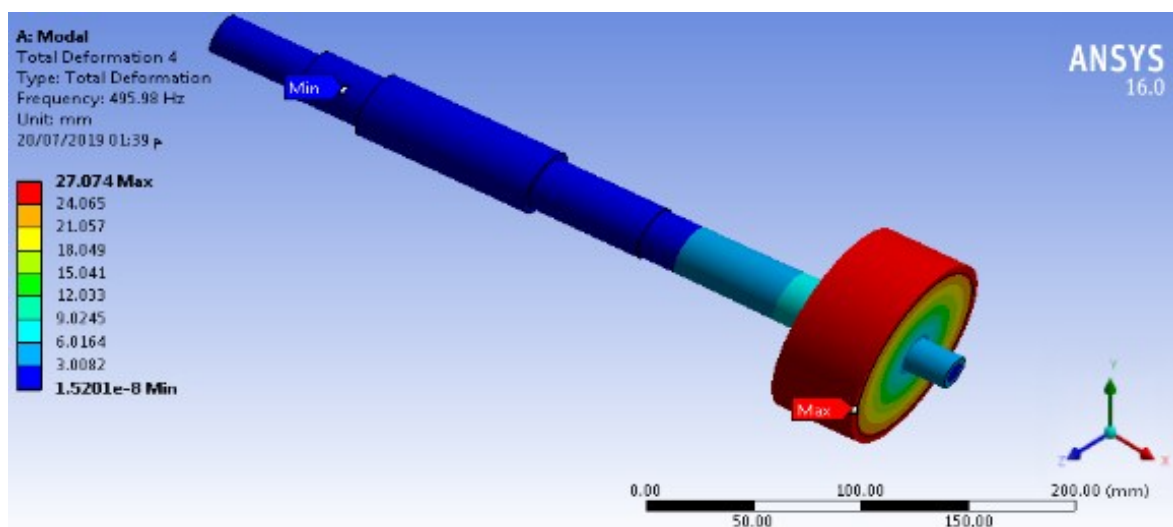
The numerical analyses of the studied model were carried out for the depths of the same cracks and as they were in the experimental work. From Figure 9, the fundamental bending natural frequency which was obtained numerically was equal to (174.64 Hz) while the corresponding experimental value was (166.65 Hz). On the other hand, the fundamental torsional natural frequency was found numerically to be equal to (495.98 Hz) while it was (465.76 Hz) experimentally as shown in Figure 10. The numerical results show a good correlation with the experimental results where the standard deviation of the results is (10.55%) for bending frequency and is (10.51%) for torsional frequency.

This result of frequency response for stepped shaft without crack experimentally was (1.36×10^{-7} mm) as shown in Figure 11, and numerically was (1.40×10^{-7} mm) as shown in Figure 12.

The numerical analysis for the tested model was performed statically and dynamically. Statically, the maximum equivalent Von-Mises stress was about (2.0783 Mpa) and the maximum total deformation was (0.006314 mm) when applying a torque of (4.77 N.m) as shown in Figures (13 and 14). Under the same boundary conditions, the dynamic analysis was performed under the effect of sinusoidal torque ($T_0 \sin(\omega t)$) were ($T_0=4.77$ N.m) during a period of analysis of one second and a variable rotation speed of (500 to 3000) rpm. Table 1, shows the dynamical numerical results for the stepped shaft.

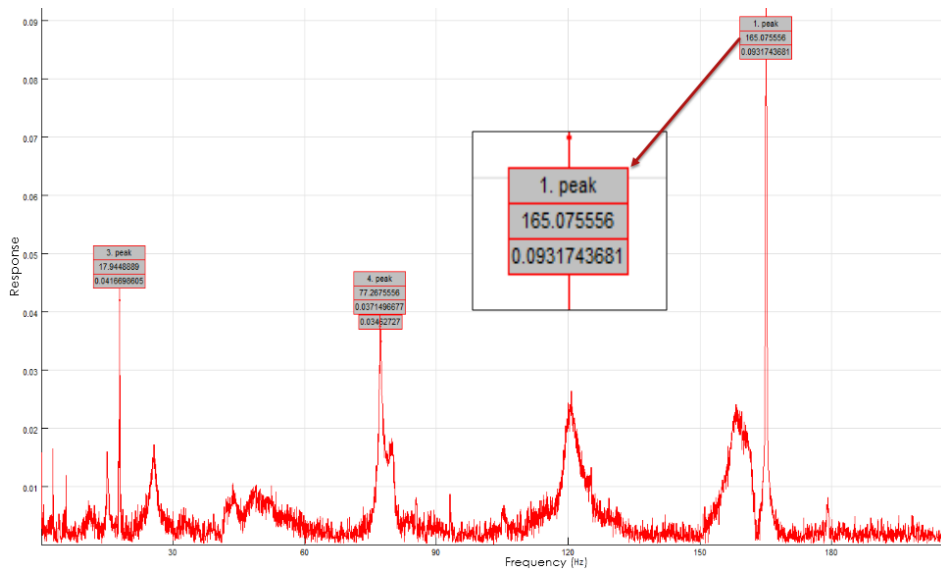


(a) Total deformation and bending natural frequency of intact shaft.

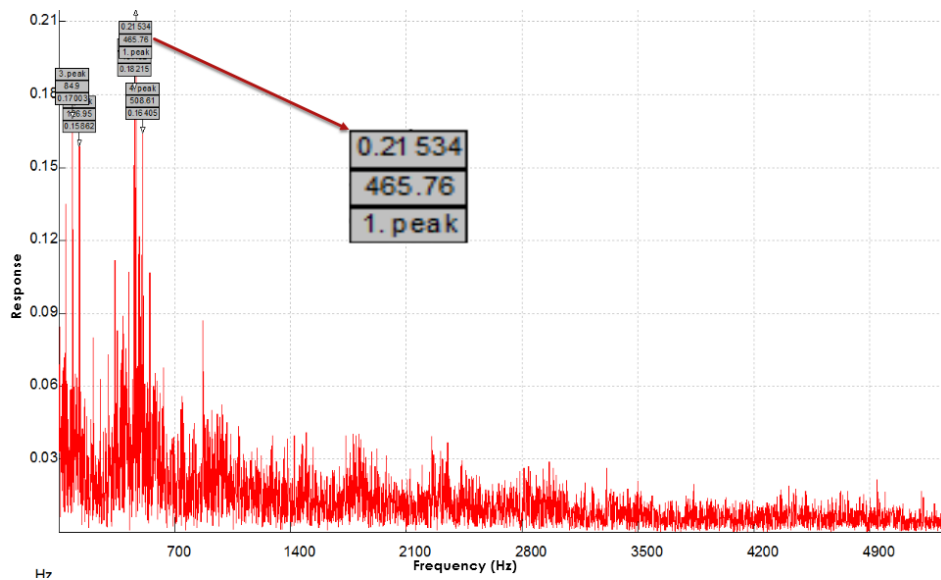


(b) Total deformation and torsional natural frequency of intact shaft.

Figure 9. Numerical analysis for the uncracked shaft.



(a) First tested position bending natural frequency.



(b) Torsional natural frequency of shaft.

Figure 10. Experimental analysis for the uncracked shaft.

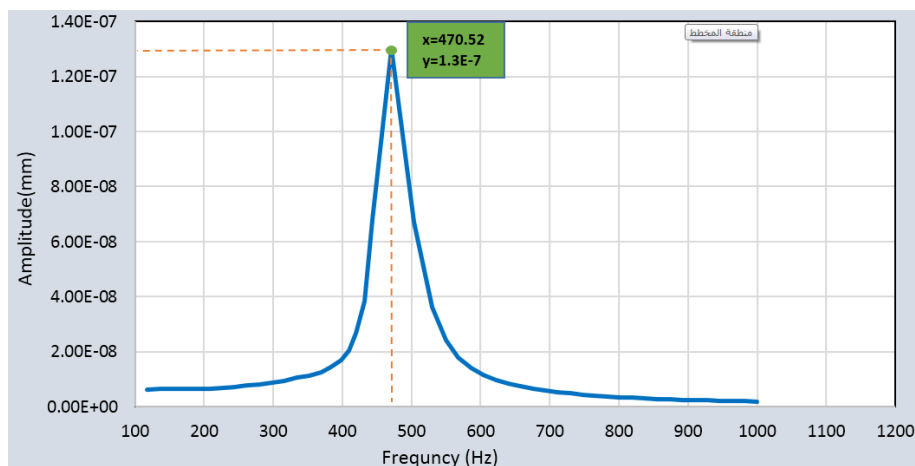


Figure11. Experimentally frequency response for uncracked shaft.

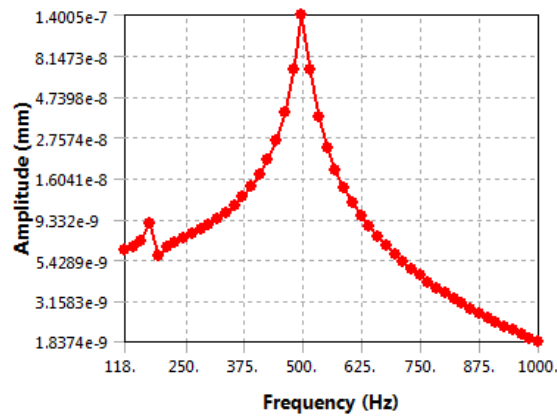


Figure 12. Numerically frequency response for uncracked shaft.

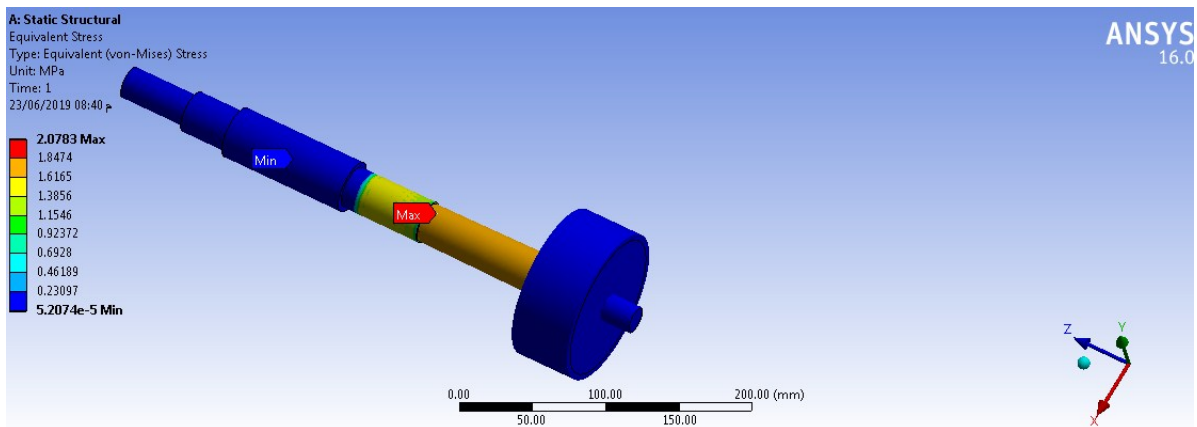


Figure 13. Equivalent (Von-Mises) stress of shaft.

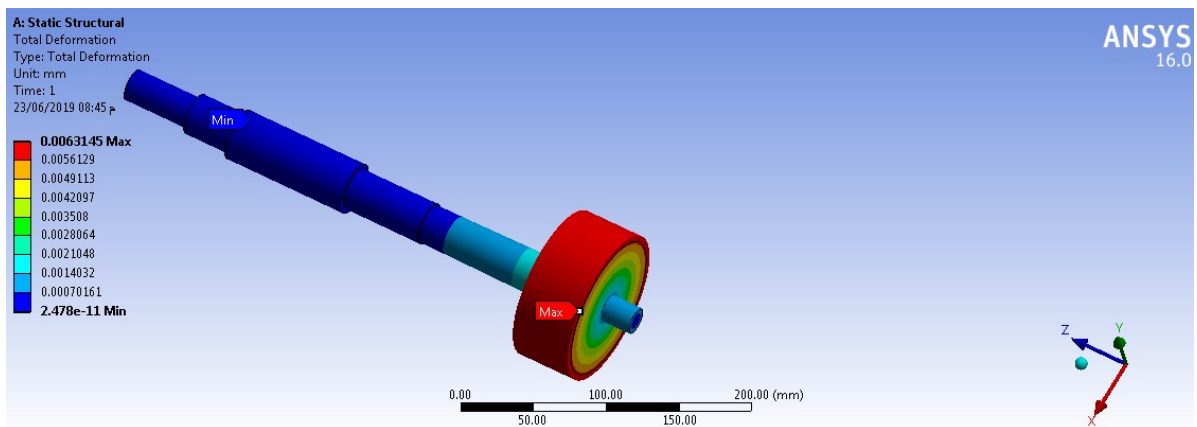


Figure 14. Total deformation of the shaft.

Table 1. Equivalent (Von-Mises) stress and total deformation at different Spin speed (N) for the stepped shaft.

Shaft speed (N)(Rpm)	Angular velocity (ω) (Rad/Sec)	Max. stress (Mpa)	Max. total deformation (mm)
500	52.360	3.3868	0.0063648
1000	104.720	3.3882	0.0063674
1500	157.080	3.3869	0.0063648
2000	209.440	3.3865	0.0063642
2500	261.800	3.3856	0.0063623
3000	314.160	3.3951	0.0063806

The dynamic load factor (DLF) is that the magnitude related between the dynamic and static stresses. It was found to be equal to (1.64) since the maximum dynamic stress for the tested stepped shaft was about 3.41MPa while the maximum static stress was about 2.08 MPa.

4.2 Results for cracked stepped shaft

The natural frequencies in both bending and torsion cases were calculated for the same shaft in the case of cracks presence numerically and experimentally. The effect of the depth of the cracks and their locations at the natural frequencies of the tested shaft was very clear through the results shown in Figure 15. The cracks will result in a significant reduction in the bending and torsional natural frequencies due to their negative impact on the stiffness of the shaft. On the other hand, changing the positions of the cracks also affects the lateral natural frequency of the shaft since the equivalent stress is a function of the cracks positions.

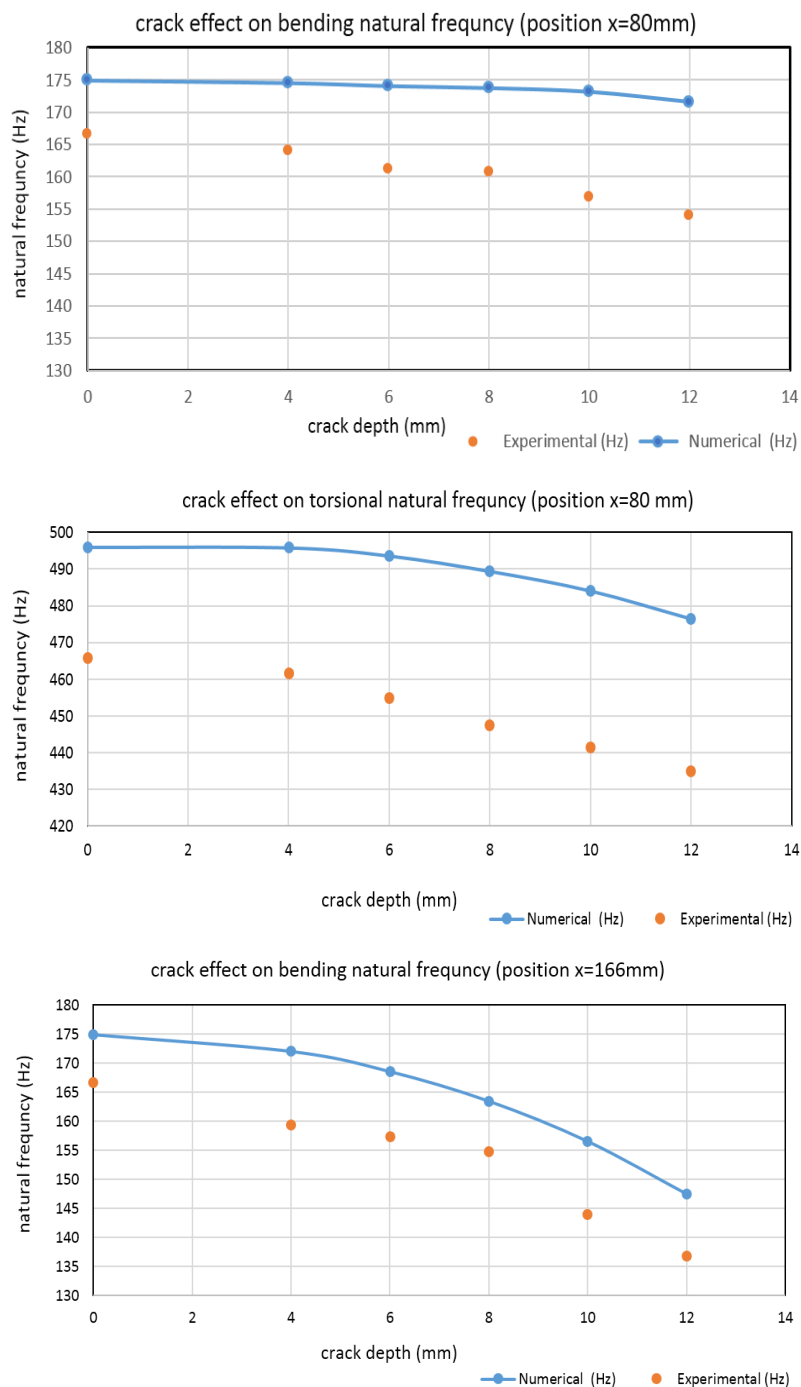


Figure 15. Continued.

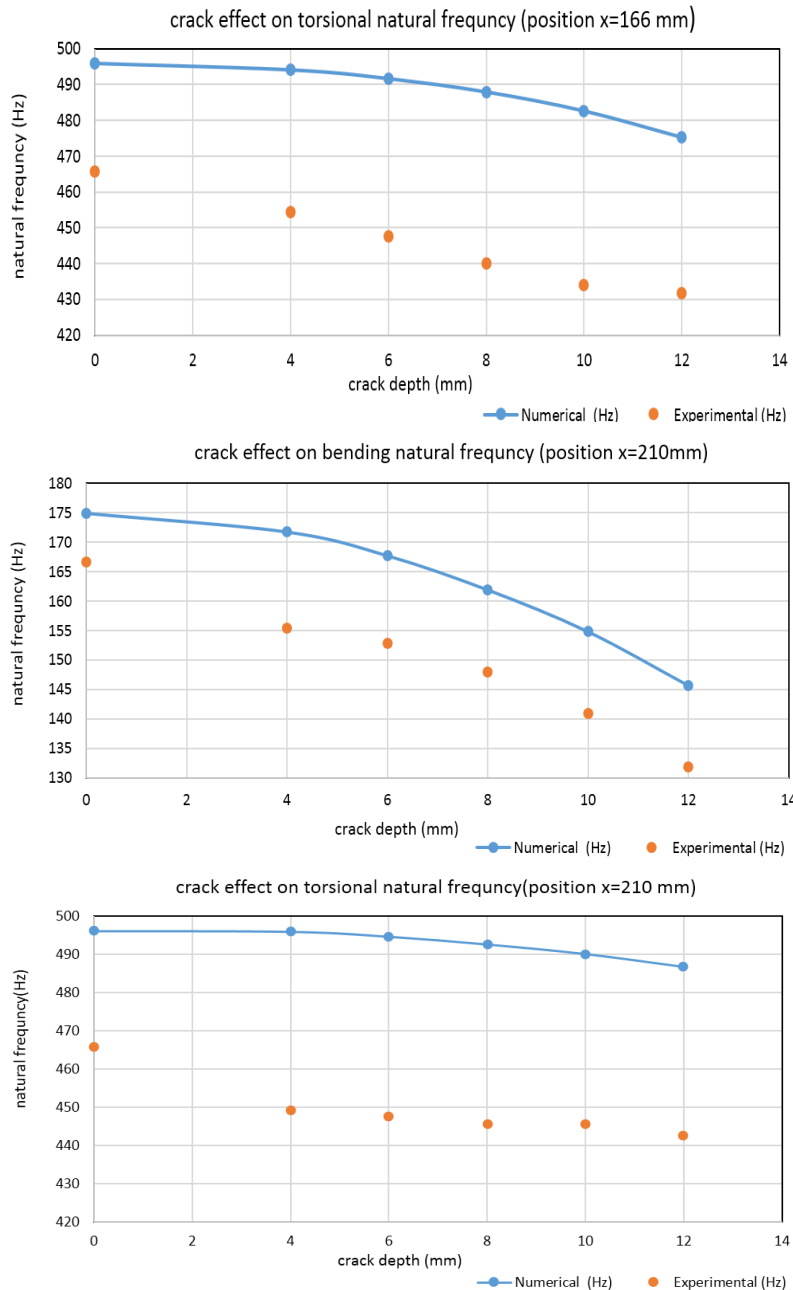


Figure 15. Comparison between experimental and numerical results for both (bending and torsional) natural frequency for the cracked stepped shaft.

The experimental frequency response for stepped shaft with a crack at ($cd=12\text{mm}$) and position ($x=166\text{mm}$) can be noted is (1.21×10^{-7}) in Figure 16, while the same response was obtained numerically is (1.245×10^{-7}) as shown in Figure 17. As the crack depths increase, the response will be increased and the critical speed will decrease. When the displacement response increases from 26% to 33% and the critical speed dropped from 15% to 20%, the crack was 0.8R which is approximately equal to (12mm).

Statically, the maximum equivalent stress (Von-Mises) was (3.3093Mpa) and the maximum total deformation was (0.0063356mm) at ($dc=4\text{mm}$, $x=166\text{mm}$). For the same crack depth but when the crack locations changed to ($x=80\text{mm}$ and $x=210\text{mm}$), the values of the maximum equivalent stress were (3.4313Mpa and 2.8767Mpa) respectively and the corresponding maximum total deformations were (6.3322 μm and 6.3344 μm) respectively. Figures 18 and 19 show the equivalent (Von-Mises) stress and the total deformation respectively for the stepped shaft at ($dc=4\text{mm}$ and $x=80\text{mm}$).

The dynamic analyses were conducted through a period of (0 - 1 sec) with variable rotation speed (N) up to (3000 rpm). These analyses were adopted to obtain the maximum equivalent stress (Von-Mises) and the maximum total deformation for the shaft with a crack at a different position (x) and different rotational

speed (N). Figures 20 and 21, show the equivalent (Von-Mises) stress and the total deformation for the stepped shaft with crack depth ($d_c=4\text{mm}$) and position ($x=80\text{mm}$) at spin speed 3000 rpm.

The relationship between stress and deformation with the depth of the crack at different speeds of rotation can be noted through Figures (22-25). It can be noted that the stress and deformation increase with increasing the depth of the crack and increasing the rotation speed. It was clear also that the stress and deformation will increase as the location of the crack is closer to the position of the disc (impeller) at the end of the shaft.

Figures 26, and 27, respectively show the highest and lowest amount of the stress and deformation occurs in the cracked shaft during the rotation at a variable speed during the same period of time (1 second) at crack position is (166mm) and spin speed (500rpm).

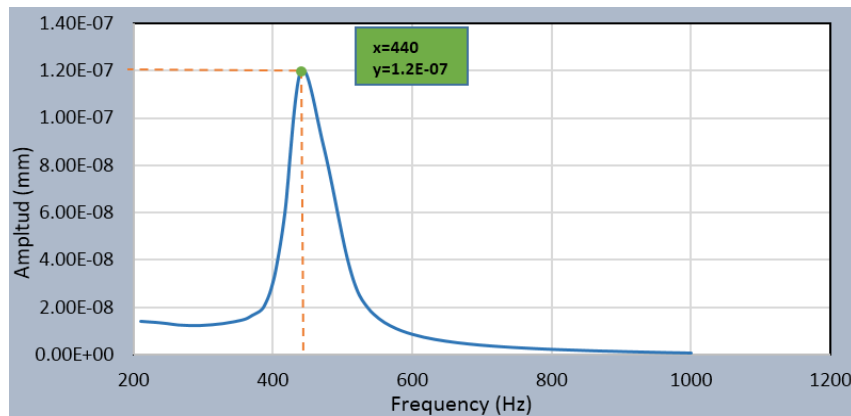


Figure 16. Experimentally frequency response for cracked shaft.

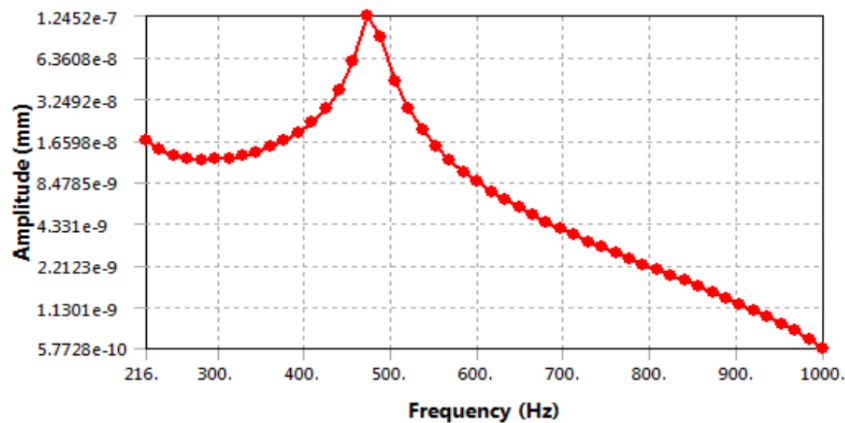


Figure 17. Numerically frequency response for cracked shaft.

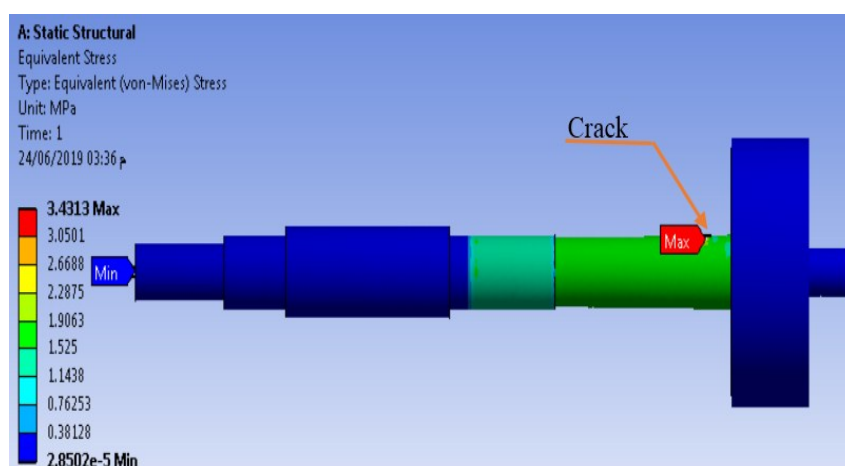


Figure 18. Equivalent stress of cracked shaft at ($d_c=4\text{mm}$, $x=80\text{mm}$).

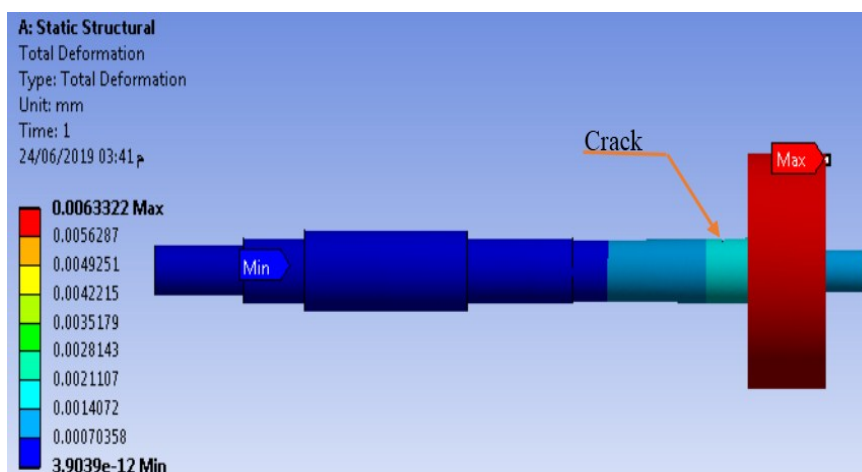


Figure 19. Total deformation of cracked shaft at ($d_c=4\text{mm}$, $x=80\text{mm}$).

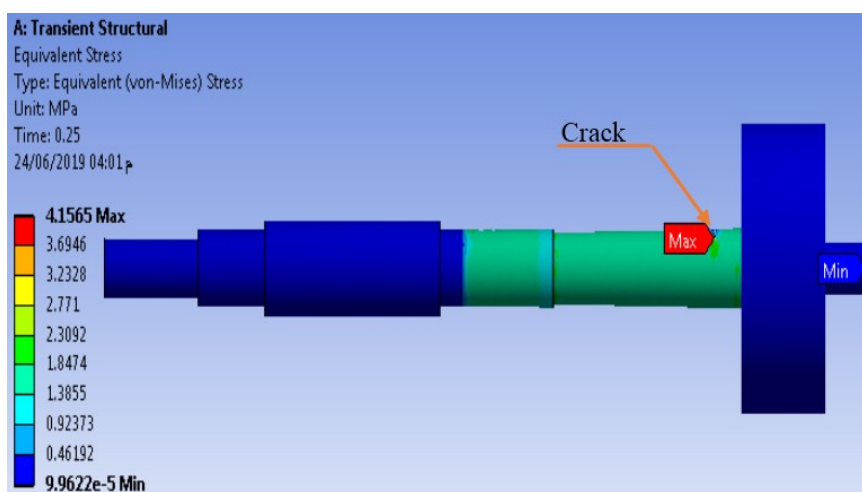


Figure 20. Maximum equivalent stress at $d_c=4\text{mm}$, $x=80\text{mm}$) and Spin speed (3000 rpm).

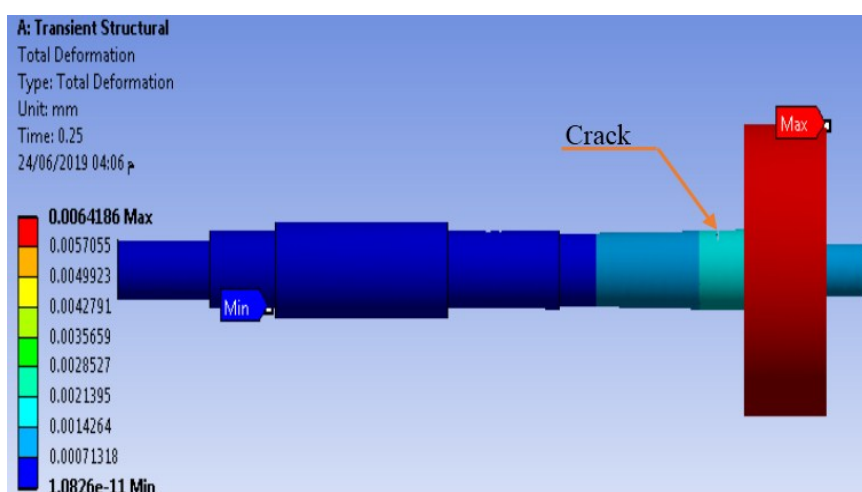


Figure 21. Maximum total deformation at (($d_c=4\text{mm}$, $x=80\text{mm}$) and Spin speed (3000 rpm).

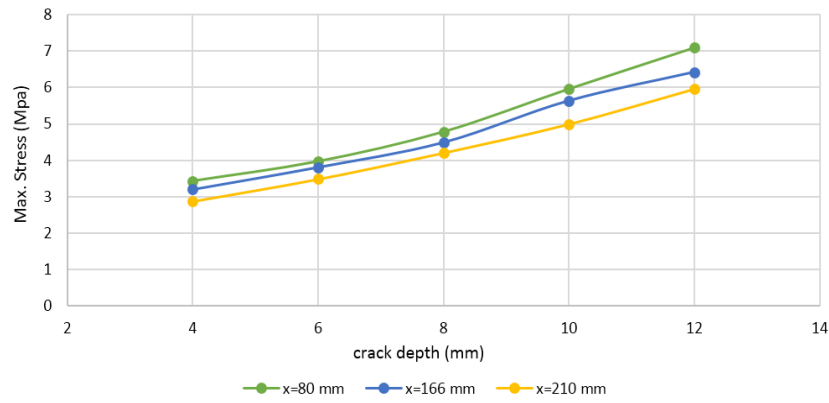


Figure 22. Statically (Von-Mises) stress of cracked shaft.

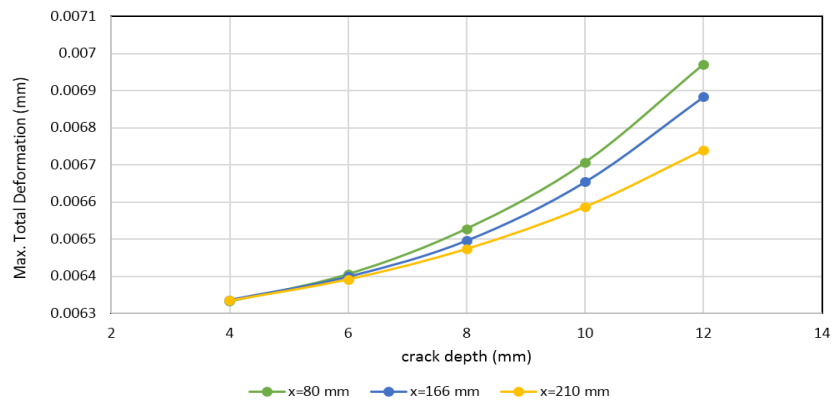


Figure 23. Statically total deformation of cracked shaft.

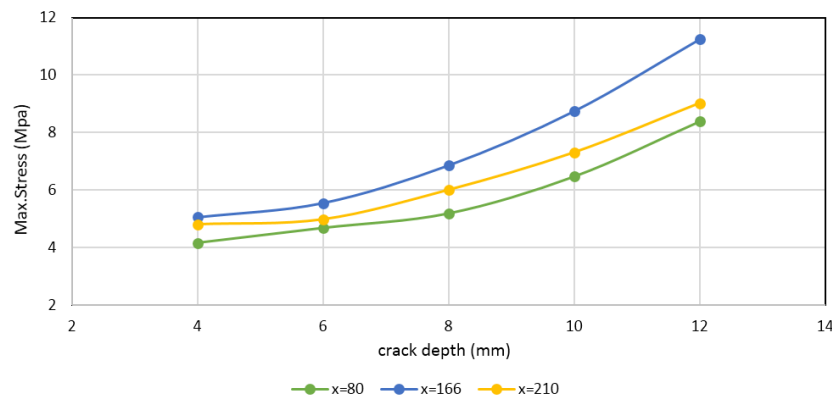


Figure 24. Dynamically (Von-Mises) stress of cracked shaft at spin speed (500rpm).

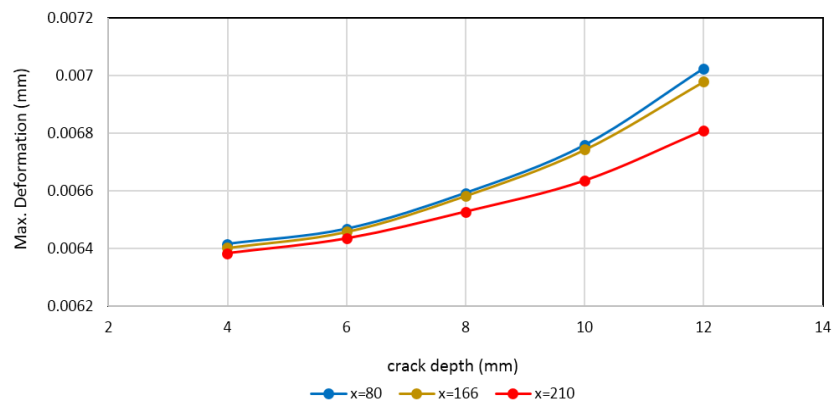


Figure 25. Dynamically total deformation of cracked shaft at spin speed (500rpm).

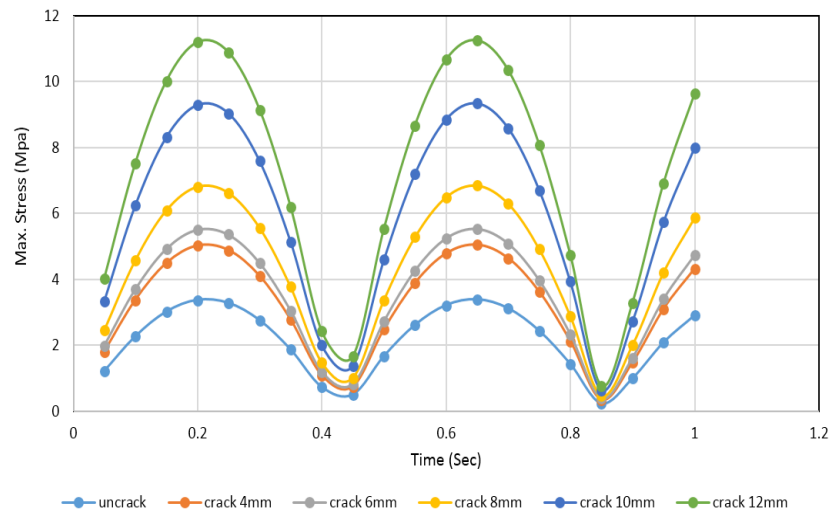


Figure 26. The stress-time curve at position (166mm) and spin speed (500rpm).

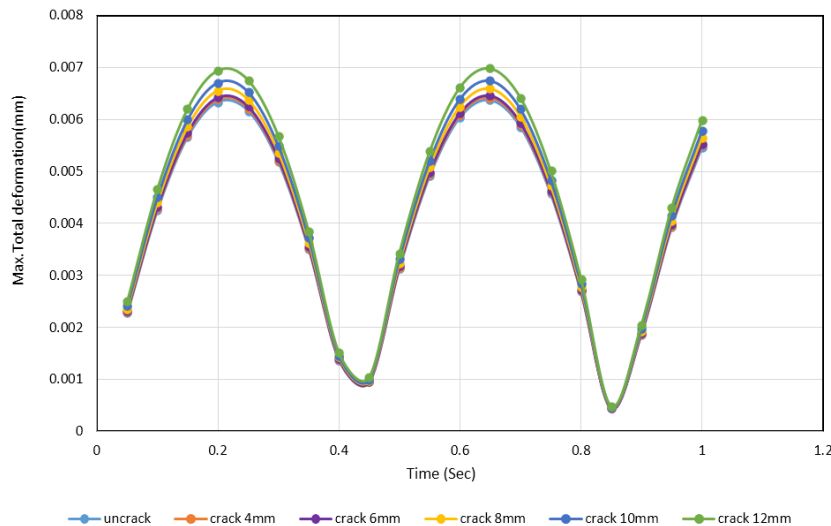


Figure 27. The deformation-time curve at position (166mm) and spin speed (500rpm).

5. Conclusion

1. Preventive maintenance at the initial installation of the shaft by setting a maintenance schedule to record the data about cracks and their growth during certain time periods.
2. The dynamic load factor (DLF) is a good crack dimension indicator. As the crack depth increases, the DLF will increase.
3. The response increases and the critical speed and natural frequency decrease as crack depths increase. If the response increases from 26% to 33% and the critical speed dropped from 15% to 20%, the fraction will be 0.8R which represents the maximum depth at the breaking point.
4. The equivalent stresses and deformations increase with increasing the crack depths and they will increase as the location of cracks will be closer to the location of the impeller mass.
5. The fundamental natural frequency will be decreased when the depths of cracks increase.

References

- [1] N.Bachschmid, R.Pennacchi, E.Tanzi, "Cracked rotors, a survey on static and dynamic behavior including modeling and diagnosis", ISBN 978-3-624-01484-0, @2010 Springer-Verlag Berlin Heidelberg.
- [2] E. Swanson, C. D. Powell & S. Weissman, "A practical review of rotating machinery critical speeds and modes", Sound and Vibration 39 (5) (2005) 10-17.
- [3] J. Vance, F. Zeidan & B. Murphy, "Machinery vibration and rotor dynamics" John Wiley & Sons, Inc., (2010).

- [4] C. Kumar, V. Rastogi “Vibration analysis of multi-rotor system through extended Lagrangian formalism”, World Journal of Modeling and Simulation, Vol. 8 No. 2, pp. 103-110 2012.
- [5] S. D. Katekar and Hemant G. Waikar, “Vibration Analysis of Rotating Shaft with Transverse Crack “, International Journal of Engineering Research & Technology (IJERT), ISSN: 2278-0181, Vol. 3 Issue 5, May – 2014, pp 1574-1578.
- [6] S. Y. Yoon, Z. Lin& P. E. Allaire “Control of Surge in Centrifugal Compressors by Active Magnetic Bearings “Springer, 2011.
- [7] M. L. Adams “Rotating Machinery Vibration, From Analysis to Troubleshooting“, Second edition Taylor & Francis Group, (2010).
- [8] R. Tiwari” A Brief History and State of the Art of Rotor Dynamics” Short Term Course on Theory & Practice of Rotor Dynamics’ ndian Institute of Technology Guwahati, 2008.
- [9] M. J. Patil and Ali Vaziri, 2013, “Vibration analysis of a cracked shaft“, University College of Engineering, India, International Journal of Advanced Engineering Technology, E-ISSN 0976-3945, IJAET/Vol. IV/ Issue II/April-June, 2013/103-104.
- [10] Muhannad Al-Waily ‘Theoretical and Numerical Vibration Study of Continuous Beam with Crack Size and Location Effect “, International Journal of Innovative Research in Science, Engineering and Technology, Vol. 2, Issue 9, September 2013, pp 4166-4177.
- [11] Muhsin J. Jweeg, Mahmud R. Ismail and Zainab M. Hwady, “Theoretical and Experimental Investigation of the Dynamical Behaviour of Complex Configuration Rotors“, Journal of Engineering, Number 2, Volume 20, February 2014, pp106-117.
- [12] Muhsin J. Jweeg, Mahmood R. Ismail and Ahmad. A. Anoze ,2012, “An Alternative Approach for Evaluating the Natural Frequencies of Elastic Rotors“, The First National Conference on Engineering and science, Fenc12, AL-Nahrain University, College of Engineering, 5-7 Nov 2012.
- [13] Ayad M. Takhakh, Fahad M. Kadhim, Jumaa S. Chiad ‘Vibration Analysis and Measurement in Knee Ankle Foot Orthosis for Both Metal and Plastic KAFO Type’ ASME 2013 International Mechanical Engineering Congress and Exposition IMECE2013, November 15-21, San Diego, California, USA, 2013.
- [14] Mohsin Abdullah Al-Shammari ‘Experimental and FEA of the Crack Effects in a Vibrated Sandwich Plate’ Journal of Engineering and Applied Sciences, Vol. 13, No. 17, pp. 7395-7400, 2018.
- [15] H. J. Abbas, M. J. Jweeg, Muhannad Al-Waily, Abbas Ali Diwan ‘Experimental Testing and Theoretical Prediction of Fiber Optical Cable for Fault Detection and Identification’ Journal of Engineering and Applied Sciences, Vol. 14, No. 02, pp. 430-438, 2019.
- [16] Bashar A. Bedaiwi , 2013 , “Analyzing of Impact, Vibration Response and Stability of Artificial Upper Limb“, American Society of Mechanical Engineering, ASME 2013 International Mechanical Engineering Congress and Exposition, Biomedical and Biotechnology Engineering, Vol. 3B.
- [17] Abdulkareem A. Alhumdany, Muhannad Al-Waily and Mohammed H. K. Al-Jabery, 2016, “Theoretical and Experimental Investigation of Using Date Palm Nuts Powder into Mechanical Properties and Fundamental Natural Frequencies of Hyper Composite Plate “, International Journal of Mechanical & Mechatronics Engineering IJMME-IJENS, Vol. 16, No. 01.
- [18] Muhsin J. Jweeg and S. Z. Said, 1995, “Effect of rotational and geometric stiffness matrices on dynamic stresses and deformations of rotating blades “, Journal of the Institution of Engineers (India): Mechanical Engineering Division, Vol. 76, pp. 29-38.
- [19] Muhannad Al-Waily, Kadhim K. Resan, Ali H. Al-Wazir and Zaman A. Abud Ali, 2017, “Influences of Glass and Carbon Powder Reinforcement on the Vibration Response and Characterization of an Isotropic Hyper Composite Materials Plate Structure “, International Journal of Mechanical & Mechatronics Engineering IJMME-IJENS, Vol. 17, No. 06.
- [20] Mohsin Abdullah Al-Shammari, Muhannad Al-Waily ‘Theoretical and Numerical Vibration Investigation Study of Orthotropic Hyper Composite Plate Structure’ International Journal of Mechanical & Mechatronics Engineering IJMME-IJENS, Vol. 14, No. 06, 2014.
- [21] Muhsin J. Jweeg, Muhannad Al-Waily, Alaa Abdulzahra Deli ‘Theoretical and Numerical Investigation of Buckling of Orthotropic Hyper Composite Plates’ International Journal of Mechanical & Mechatronics Engineering IJMME-IJENS, Vol. 15, No. 04, 2015.
- [22] Mohsin Abdullah Al-Shammari, Muhannad Al-Waily ‘Analytical Investigation of Buckling Behavior of Honeycombs Sandwich Combined Plate Structure’ International Journal of Mechanical and Production Engineering Research and Development (IJMPERD), Vol. 08, No. 04, pp. 771-786, 2018.

- [23] Jumaa S. Chiad, Muhannad Al-Waily, Mohsin Abdullah Al-Shammari 'Buckling Investigation of Isotropic Composite Plate Reinforced by Different Types of Powders' International Journal of Mechanical Engineering and Technology (IJMET), Vol. 09, No. 09, pp. 305–317, 2018.
- [24] Mahmud Rasheed Ismail, Zaman Abud Almalik Abud Ali, Muhannad Al-Waily 'Delamination Damage Effect on Buckling Behavior of Woven Reinforcement Composite Materials Plate' International Journal of Mechanical & Mechatronics Engineering IJMME-IJENS, Vol. 18, No. 05, pp. 83-93, 2018.
- [25] Muhannad Al-Waily, Emad Q. Hussein, Nibras A. Aziz Al-Roubaiee 'Numerical Modeling for Mechanical Characteristics Study of Different Materials Artificial Hip Joint with Inclination and Gait Cycle Angle Effect' Journal of Mechanical Engineering Research & Developments (JMERE), Vol. 42, No. 04, pp. 79-93, 2019.
- [26] Muhsin J. Jweeg, Sameer Hashim Ameen 'Experimental & theoretical investigations of dorsiflexion angle and life of an ankle-Foot-Orthosis made from (Perlon-carbon fibre-acrylic) and polypropylene materials' 10th IMEKO TC15 Youth Symposium on Experimental Solid Mechanics, 2011.
- [27] Muhsin J. Jweeg, Kadhim K. Resan, Mustafa Tariq Ismail 'Study of Creep-Fatigue Interaction in a Prosthetic Socket below Knee' ASME International Mechanical Engineering Congress and Exposition, 2012.
- [28] Muhsin J. Jweeg, A. A. Alhumandy, H. A. Hamzah 'Material Characterization and Stress Analysis of Openings in Syme's Prosthetics' International Journal of Mechanical & Mechatronics Engineering IJMME-IJENS, Vol. 17, No. 04, 2017.
- [29] Mohsin Abdullah Al-Shammari, Emad Q. Hussein, Ameer Alaa Oleiwi 'Material Characterization and Stress Analysis of a Through Knee Prosthesis Sockets' International Journal of Mechanical & Mechatronics Engineering IJMME-IJENS, Vol. 17, No. 06, 2017.
- [30] Saif M. Abbas, Ayad M. Takhakh, Mohsin Abdullah Al-Shammari, Muhannad Al-Waily 'Manufacturing and Analysis of Ankle Disarticulation Prosthetic Socket (SYMES)' International Journal of Mechanical Engineering and Technology (IJMET), Vol. 09, No. 07, pp. 560-569, 2018.
- [31] Saif M. Abbas, Kadhim K. Resan, Ahmed K. Muhammad, Muhannad Al-Waily 'Mechanical and Fatigue Behaviors of Prosthetic for Partial Foot Amputation with Various Composite Materials Types Effect' International Journal of Mechanical Engineering and Technology (IJMET), Vol. 09, No. 09, pp. 383–394, 2018.
- [32] Muhsin J. Jweeg, Muhannad Al-Waily, Ahmed K. Muhammad, Kadhim K. Resan 'Effects of Temperature on the Characterisation of a New Design for a Non-Articulated Prosthetic Foot' IOP Conference Series: Materials Science and Engineering, Vol. 433, 2nd International Conference on Engineering Sciences, Kerbala, Iraq, 26–27 March, 2018.
- [33] Muhsin J. Jweeg, 1983, "Application of finite element analysis to rotating fan impellers", Doctoral Thesis, Aston University.
- [34] Ehab N. Abbas, Muhsin J. Jweeg and Muhannad Al-Waily, 2018, "Analytical and Numerical Investigations for Dynamic Response of Composite Plates Under Various Dynamic Loading with the Influence of Carbon Multi-Wall Tube Nano Materials ", International Journal of Mechanical & Mechatronics Engineering IJMME-IJENS, Vol. 18, No. 06, pp. 1-10.
- [35] Mohsin Abdullah Al-Shammari, Lutfi Y. Zedan, Akram M. Al-Shammari 'FE simulation of multi-stage cold forging process for metal shell of spark plug manufacturing' 1st International Scientific Conference of Engineering Sciences-3rd Scientific Conference of Engineering Science, ISCES 2018–Proceedings, 2018.
- [36] Muhsin J. Jweeg, Zaid S. Hammoudi, Bassam A. Alwan 'Optimised Analysis, Design, and Fabrication of Trans-Tibial Prosthetic Sockets' IOP Conference Series: Materials Science and Engineering, 2nd International Conference on Engineering Sciences, Vol. 433, 2018.
- [37] Ayad M. Takhakh, Saif M. Abbas 'Manufacturing and Analysis of Carbon Fiber Knee Ankle Foot Orthosis' International Journal of Engineering & Technology, Vol. 07, No. 04, pp. 2236-2240, 2018.
- [38] Ahmed A. Taher, Ayad M. Takhakh, Sabah M. Thaha 'Experimental Study and Prediction the Mechanical Properties of Nano-Joining Composite Polymers' Journal of Engineering and Applied Sciences, Vol. 13, No. 18, pp. 7665, 7669, 2018.

Muhsin. J. Jweeg muhsinjj@gmail.com

Salah. N. Alnomani salah.n@uokerbala.edu.iq

Salah. K. Mohammad 200saaa200@gmail.com